JGR Atmospheres

RESEARCH ARTICLE
10.1029/2021JD034754

# The Influence of Atmospheric Rivers on Cold-Season Precipitation in the Upper Great Lakes Region

**Marian E. Mateling[1], Claire Pettersen[2], Mark S. Kulie[3], Kyle S. Mattingly[4], Stephanie A. Henderson[1], and Tristan S. L'Ecuyer[1]**

[1]Department of Atmospheric and Oceanic Sciences, University of Wisconsin-Madison, Madison, WI, USA, [2]Space Science and Engineering Center, University of Wisconsin-Madison, Madison, WI, USA, [3]NOAA/NESDIS/Center for Satellite Applications and Research, Advanced Satellite Products Branch, Madison, WI, USA, [4]Institute of Earth, Ocean, and Atmospheric Sciences, Rutgers University, New Brunswick, NJ, USA

**Key Points:**

- Deep, synoptically forced cold-season precipitation is frequently associated with atmospheric rivers (ARs) in the Upper Great Lakes region
- Precipitation rates are enhanced and rain is four times more likely to occur than snow if an AR is proximal
- Upper Great Lakes ARs are significantly correlated to negative phases of the Pacific-North American pattern and Pacific Decadal Oscillation

**Correspondence to:**
M. E. Mateling,
mateling@wisc.edu

**Citation:**
Mateling, M. E., Pettersen, C., Kulie, M. S., Mattingly, K. S., Henderson, S. A., & L'Ecuyer, T. S. (2021). The influence of atmospheric rivers on cold-season precipitation in the Upper Great Lakes region. *Journal of Geophysical Research: Atmospheres*, *126*, e2021JD034754. https://doi.org/10.1029/2021JD034754

Received 10 FEB 2021
Accepted 21 JUN 2021



**Abstract** This study aims to identify the impacts of atmospheric rivers (AR) associated with cold-season precipitation in the Upper Great Lakes region of the United States. A MERRA-2-derived AR dataset is combined with data from a suite of instruments hosted by the National Weather Service in Marquette, Michigan, including a profiling radar and a video disdrometer. ARs coincide with deep, synoptically-forced precipitation 28% of the time during the cold season. These ARs are found to intrude from the southwest and are associated with warmer surface and upper-level temperatures, increased radar reflectivity values, and enhanced precipitation rates. Warmer atmospheric temperatures aloft associated with ARs lead to a fourfold increase in the likelihood that cold-season precipitation will be rain instead of snow. Additionally, inland ARs in the Upper Great Lakes region are correlated with the negative phases of the Pacific Decadal Oscillation and the Pacific-North American pattern.

**Plain Language Summary** The Upper Great Lakes region of the United States experiences an abundance of snowfall each year. The National Weather Service in Marquette, Michigan closely monitors snowfall events due to the socioeconomic impact on the surrounding communities. Studies have shown that intrusions of enhanced levels of atmospheric water vapor, or "atmospheric rivers", lead to increased precipitation along oceanic coastlines and other parts of the interior United States. This study investigates the impact of atmospheric rivers on cold-season precipitation in the Upper Great Lakes region using ground-based observations from Marquette. We find that atmospheric rivers occur frequently during large-scale, deep precipitation events and are associated with enhanced precipitation rates, greater likelihood of rain instead of snow at the surface, and warmer temperatures. These events are also correlated with well-known climate variability patterns, which could aid forecasters in mid- and long-range prediction of these weather events.

## 1. Introduction

Cold season precipitation is a vital component of the hydrological cycle in the Great Lakes region. Rain and snow events during the winter season impact agriculture, ecosystems, travel, and water management, and can be hazardous to life and property (Bolsenga & Norton, 1992; Changnon, 1979; Norton & Bolsenga, 1993; Riebsame et al., 1986). Winter rainfall that occurs on top of snowpack, called rain-on-snow, can lead to snowmelt and subsequent flooding (Guan et al., 2016; McCabe et al., 2007). This is especially problematic, as warming in the Great Lakes region due to climate change is expected to result in loss of snowpack, increased rainfall intensity, and increased risk of flooding (Byun et al., 2019).

Atmospheric rivers (ARs), defined as locally enhanced transport of large amounts of water vapor, have been shown to exert a strong influence on cold-season precipitation. Several studies have documented the impacts of ARs on precipitation amounts in the western U.S. (e.g., Guan et al., 2012, 2013; Neiman et al., 2008; Rivera et al., 2014; Warner et al., 2012) and southeastern U.S. (Mahoney et al., 2016; Miller et al., 2018; Moore et al., 2012). In the Midwest U.S., a few studies have linked ARs to extreme precipitation (Slinskey et al., 2020) and winds (Waliser & Guan, 2017), but there is a lack of detailed examination of the Great Lakes region in particular. Additionally, the influence of ARs on precipitation phase is incompletely understood and AR impacts on precipitation phase and snowpack vary regionally and cannot be applied globally. In

the Sierra Nevada mountain range, Guan et al. (2016) found that rain-on-snow and snowmelt occurred in 15% of AR events. Goldenson et al. (2018) found that increased AR frequency correlated with increased winter snowpack in the Sierra Nevada, but decreased winter snowpack in the Cascade Mountains. High latitude ARs, such as in Alaska, have been found to increase rain and flooding (Papineau & Holloway, 2012; Mundhenk et al., 2016). Comparatively fewer studies have examined the impact of ARs on precipitation and snowpack in inland regions. Rutz et al. (2014) found that AR frequency in the interior western U.S. is related to the frequency of landfalling ARs on the west coast. Inland ARs have been linked to heavier precipitation and flooding in the central U.S. (Lavers & Villarini, 2013; Nayak et al., 2016) and landslides in the Appalachian Mountains (Miller et al. 2019). In this work, we extend these previous analyses of inland AR impacts to the Upper Great Lakes region, located in the northern mid-latitudes.

AR frequency and intensity and associated precipitation have been linked to climate signals, and the relationship between these signals and ARs varies by region. In the Sierra Nevada, for example, anomalous AR frequency is associated with the Madden-Julian Oscillation (MJO; Guan et al., 2012) and joint negative phases of the Arctic Oscillation (AO) and Pacific-North American (PNA) pattern (Guan et al., 2013; Guan & Waliser, 2015). Likewise, Lavers and Villarini (2013) connected AR-related flood events in the central U.S. and the negative phase of the PNA. Connecting AR activity to these climate signals can aid in predicting when and where they occur, and consequently improve forecasts of extreme precipitation events. Globally, the socio-economic impact of ARs is both costly and hazardous and therefore requires better understanding and prediction (Waliser & Guan, 2017).

Located in Michigan's Upper Peninsula on the southern shore of Lake Superior, Marquette (46.5°N, 87.4°W) frequently experiences shallow, lake-effect precipitation in addition to deeper, synoptically-driven precipitation during winter. Both types of precipitation contribute equally to wintertime snow accumulation, despite synoptically-driven precipitation occurring half as often as lake-effect precipitation (Pettersen, Kulie, et al., 2020). In collaboration with the National Aeronautics and Space Administration's (NASA) Wallops Flight Facility and Goddard Flight Facility, the National Weather Service (NWS) in Marquette has served as a ground-based instrument site since 2014. The site serves as one of few long-duration field campaigns studying snowfall processes, and the data collected at this site can be treated as representative of the Upper Great Lakes region as a whole.

Due to its location far inland in the northern U.S., the Great Lakes region experiences relatively dry atmospheric conditions during the Northern Hemisphere winter. Examining the influence of Great Lakes ARs during the cold-season therefore requires an identification scheme that is sensitive to lower values of integrated water vapor transport. This type of AR identification was demonstrated by Gorodetskaya et al. (2014) in Eastern Antarctica and Mattingly et al. (2018) in Greenland. Gorodetskaya et al. (2014) found that ARs landfalling in Eastern Antarctica led to high-accumulation precipitation events, while Mattingly et al. (2018) found that ARs in Greenland led to accelerated surface ice sheet melt during the warm season. The presented work will use a dataset of ARs created by Mattingly et al. (2018) and leverage a suite of long-duration instrument-based observations of snow in Marquette (Kulie et al., 2021; Pettersen, Kulie, et al., 2020) to examine the impact that ARs have on cold-season precipitation in the Upper Great Lakes region.

## 2. Data and Methods

The National Weather Service (NWS) office in Marquette, Michigan hosts several instruments that collect meteorological measurements, including surface temperature (2-meter), wind speed, and wind direction (10-meter). In January 2014, a Micro-Rain Radar 2 (MRR) and Precipitation Imaging Package (PIP) were installed at the Marquette NWS to provide radar and precipitation observations year-round. In addition to providing power, staff at the NWS occasionally services the instruments as needed. These instruments provide near-real-time observations of precipitation in Marquette and can be monitored online at www.ssec.wisc.edu/lake_effect/mqt/.

The 24-GHz vertically-pointing MRR measures reflectivity, Doppler velocity, and Doppler spectral width (Klugmann et al., 1996). The PIP is a video disdrometer that takes images of falling particles and provides particle size distributions, fall speeds, and precipitation rates (A. J. Newman et al., 2009; Pettersen, Bliven,

et al., 2020). Phase separation of PIP precipitation into rain and snow rates is available as a higher-order-derived data product (Pettersen et al., 2021), including during mixed precipitation conditions, as well as from NWS observations. The observational dataset containing MRR, PIP, and surface meteorological data is available from January 2014 to December 2019 at 1-min resolution (Pettersen, Kulie, et al., 2020). This study is limited to the cold season, defined as October through May (Note: In February 2019, a power failure of the Marquette NWS meteorological instruments necessitated substitution of temperature and wind observations using data from the Sawyer International Airport, ∼30 km away). The Marquette NWS also hosts a Next-Generation Weather Radar (NEXRAD) Doppler radar that provides Level-II base reflectivity data used in this work.

ARs are characteristically filamentary in structure and responsible for most meridional water vapor transport in the midlatitudes (Zhu & Newell, 1998). Multiple AR algorithms exist that differ based on the datasets used and definition criteria (Rutz et al., 2019). The AR identification database used for this work is from Mattingly et al. (2018), which leverages the NASA Modern-Era Retrospective analysis for Research and Applications, Version 2 reanalysis product (MERRA-2; Gelaro et al., 2017). This dataset is available at 6-hourly resolution from January 1980 to December 2019. Mattingly et al. (2018) derived integrated water vapor transport (IVT) and associated moisture transport vectors from MERRA-2. ARs are then identified using thresholds of IVT > 150 kg $m^{-1}$ $s^{-1}$ and >85th percentile rank, with additional filtering criteria designed to locate narrow plumes of poleward moisture transport (details in Mattingly et al., 2018).

To examine how ARs influence surface meteorology and precipitation microphysics in the Upper Great Lakes region, ground-based observations are matched to all ARs detected within 100 km of Marquette from January 2014 to December 2019. Though the dataset does not provide information about the AR major axis, Nayak et al. (2016) showed that most precipitation associated with ARs occurs within 100 km the axis. A one-hour window (±30 min) is applied to the observations assuming that any AR present in the database will remain in the region for at least one hour. Each time-step is classified as precipitating or not precipitating using the MRR reflectivity profile and NEXRAD Level II reflectivity. At least 25% of the hour-window must have coincident precipitation and surface temperatures <2°C to be considered. Independent precipitation events are defined when a gap of at least 12 h exists between timesteps. Events with MRR echo-tops ≥3 km above ground level (AGL) are further classified as "deep precipitation" (see details in Pettersen, Kulie, et al., 2020). We performed a difference of means test on observation comparisons and tested for significance at the 95% confidence level (Wilks, 2011).

Large-scale circulation conditions during AR-influenced deep precipitation events are examined using mean sea level pressure (MSLP) and 500 hPa geopotential height ($Z_{500}$) products from the European Centre for Medium-Range Weather Forecasts ERA5 reanalysis data set (C3S, 2017; Hersbach et al., 2020) from 1980 to 2019. MSLP and $Z_{500}$ anomalies are computed by taking each individual deep precipitation event and subtracting the monthly climatological mean. A Student's t-test is used to determine if the anomaly composites are significantly different from zero at the 95% level, where AR events are considered independent if they are at least 2 days apart. Similar results are obtained with a more conservative sample size since the majority of events are greater than one week apart. To examine the possible role of climate variability on AR frequency in the Upper Great Lakes region, correlations with various monthly climate indices were computed. The Pacific Decadal Oscillation (PDO), the PNA, the AO, and the El Niño-Southern Oscillation (ENSO) Niño 3.4 indices are all obtained from the National Oceanic and Atmospheric Administration (NOAA) Climate Prediction Center (CPC). For each climate index, a null hypothesis of zero correlation with AR frequency is tested by calculating a *t*-value and using a 95% level of certainty.

## 3. Results

### 3.1. Precipitation Event Characteristics

Over the 5 years of cold seasons examined, an AR was detected within 100 km of the Marquette observation site during 6.4% of 6-hourly timesteps. We found that an AR is present nearly twice as often (9.5%) in precipitating timesteps than non-precipitating timesteps (4.9%). However, when further distinguishing between deep (MRR echo-tops ≥3 km AGL) and shallow (MRR echo-tops <3 km AGL) events, an AR is present during only 3.9% of shallow precipitation timesteps but during 28.0% of deep precipitation timesteps. Given

**Table 1**
*Mean and Standard Deviation Meteorological Data Collected at NWS Marquette for Deep Precipitation Events When an AR is Present (Left Column) and Not Present (Right Column)*

| | Deep + AR | | Deep + No AR | |
|---|---|---|---|---|
| | Mean | Std dev | Mean | Std dev |
| Temp (°C) | **−2.99** | 3.81 | **−4.85** | 5.06 |
| Near-Surface Reflectivity (dBZ) | **15.2** | 6.22 | **12.0** | 5.98 |
| Near-Surface Doppler Velocity (m $s^{-1}$) | **1.79** | 1.18 | **1.20** | 0.72 |
| PIP Total Precip Rate (LWE; mm $hr^{-1}$) | **1.14** | 1.33 | **0.761** | 0.91 |
| Wind Speed (m $s^{-1}$) | 3.05 | 1.80 | 2.55 | 1.77 |
| PIP Rain Frequency (%) | 20.1% | | 5.74% | |

*Note*. Frequency of occurrence of PIP rain rates is included. Statistically significant differences are bolded.
Abbreviations: AR, atmospheric river; PIP, Precipitation Imaging Package.

how far inland the Upper Great Lakes region is, the presence of an AR during more than a quarter of all cold-season deep precipitating timesteps motivates further examination of the associated meteorological and synoptic conditions. During the 5-year period examined, we identified 207 independent deep precipitating events of which 58 coincided with an AR.

The mean and standard deviations of the surface meteorological, MRR, and PIP observations are shown in Table 1 for independent deep precipitation events associated with (left) and without (right) ARs. Events with ARs exhibit warmer temperatures (+1.86°C), larger near-surface MRR reflectivities (+3.2 dBZ) and Doppler velocities (+0.59 m $s^{-1}$). The difference between wind speeds is not statistically significant. We partitioned the PIP precipitation rate by phase and found that frequency of occurrence of rain is 20.1% when there is an AR present, versus 5.74% when an AR is not present: a fourfold increase in frequency. The mean PIP liquid water equivalent (LWE) rate across all deep precipitation events is significantly higher (+0.379 mm $hr^{-1}$) when an AR is present. However, when partitioned by phase, rain rates are significantly higher when an AR is present, whereas the difference between snow LWE rates is not significant.

Two-dimensional histograms of MRR reflectivity profiles are computed for the independent deep precipitation events when an AR is present versus not (Figure 1). The distribution is narrow and tightly concentrated between 15 and 20 dBZ near the surface (<1 km AGL) when an AR is present (Figure 1a). When no AR is present (Figure 1b), MRR reflectivities are broadly distributed throughout the profile with values between 5 and 20 dBZ near the surface. Histograms of MRR reflectivity and Doppler velocity values for individual AR-influenced deep precipitation events (not shown) show several instances where a melting layer is clearly identifiable.

Wind roses, illustrating the distributions of wind speed and direction, are shown in Figures 1c and 1d for independent deep precipitation events when an AR is present versus not, respectively. The wind direction is bimodal when an AR is present during deep precipitation, with south-southwesterly winds >20% of the time, and east-northeasterly winds ∼15% of the time (Figure 1c). There is no preferential wind direction when no AR is present. Notably, winds from the south-southwest are the most frequent during deep precipitation regardless of AR presence. Wind speeds do not increase significantly if an AR is present.

### 3.2. Environmental Conditions

Composite maps of AR locations leading up to and during the deep precipitation events are shown in Figure 2 for 24 h (Figure 2a) and 12 h prior to (Figure 2b), and during the event (Figure 2c). The composites show that ARs are generally located southwest and west of Marquette preceding the deep precipitation events. Figures 2d–2f show the composite IVT and associated moisture transport vectors for the same timesteps. The mean trajectory of the IVT indicates that moisture is primarily advected from the Gulf of Mexico and transported north toward Marquette through the central-eastern US.

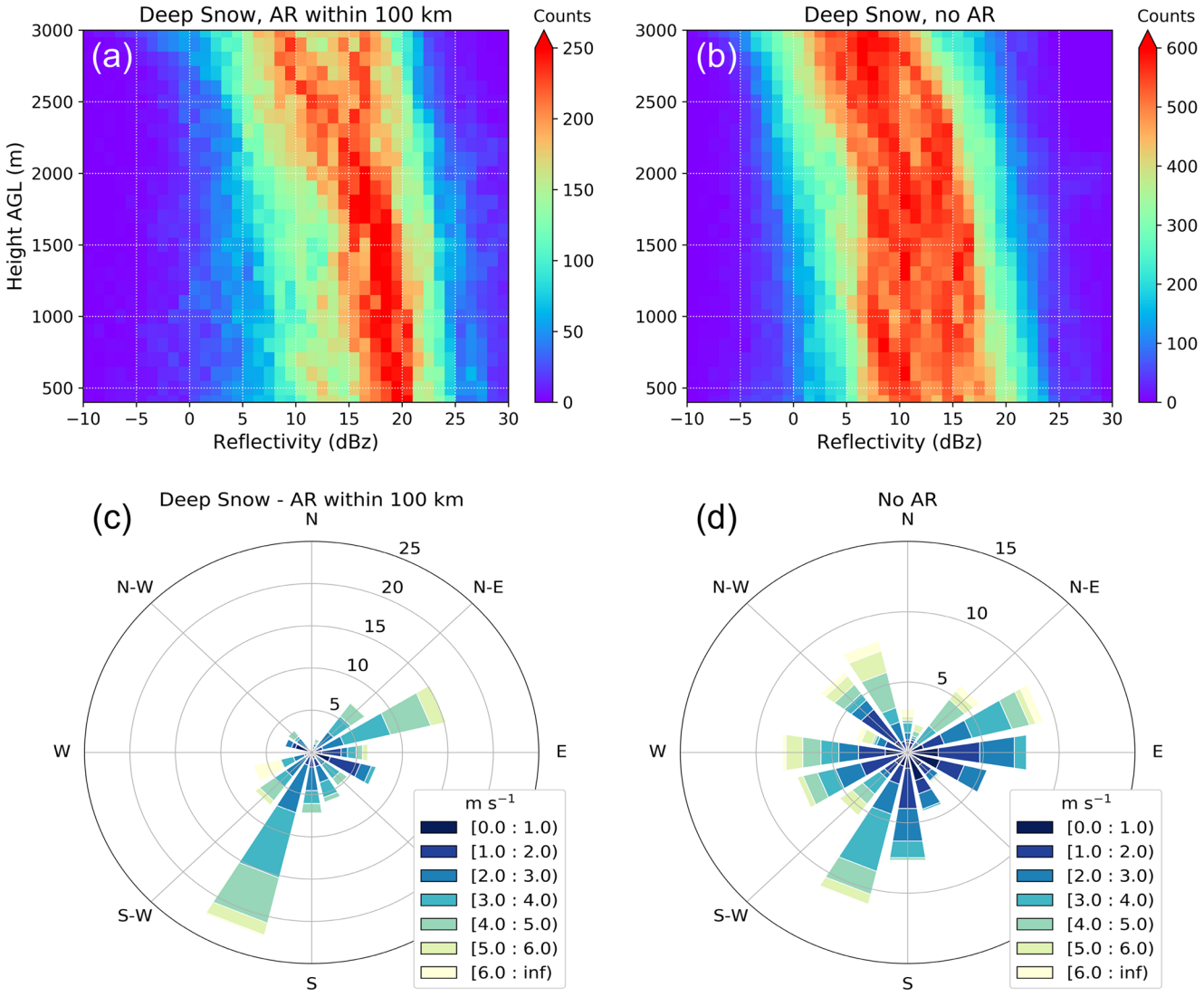


**Figure 1.** (a–b) Two-dimensional histograms of Micro-Rain Radar 2 (MRR) reflectivity profiles during deep precipitation events when an AR (a) is present and (b) is not present. The histogram bin sizes are 1 dBZ for reflectivity and 100 m for height. (c–d) Wind roses representing the distribution of wind speeds and directions when an atmospheric river (AR) (c) is present and (d) is not present. Frequency of occurrence of wind direction is represented by the concentric rings and wind speeds are represented by color.

To better understand the atmospheric conditions during the AR-enhanced deep precipitation events, we analyzed composites of the ERA5 MSLP (Figures 3a–3c) and $Z_{500}$ anomalies (Figures 3d–3f). Similar to Figure 2, the composites are relative to deep precipitation events and show conditions leading up to the event. Anomalous MSLP is negative west of Marquette and becomes progressively more anomalous as low-pressure anomalies track northeastward toward Marquette leading up to the events. To the east there is anomalously high MSLP that also amplifies over time. At $T = 0$, the average position of the negative MSLP anomalies is centered just southwest of Marquette. The $Z_{500}$ anomalies (Figures 3d–3f) indicate that in the 24 h leading up to an AR-enhanced deep precipitation event, an anomalous ridge over the Great Lakes region amplifies and travels eastward while an anomalous trough to the west propagates eastward. This type of circulation is not only characteristic of deep precipitation events, but also facilitates the southwesterly flow as found in the surface winds in Figure 1 and the IVT maps in Figure 2.

The significance of these synoptic-scale anomalies during these AR-enhanced deep precipitation events indicates that climate variability may play a role. We find that cold-season ARs within 100 km of Marquette from 1980 to 2019 are more frequent during the negative phases of the PNA (Wallace & Gutzler, 1981) and

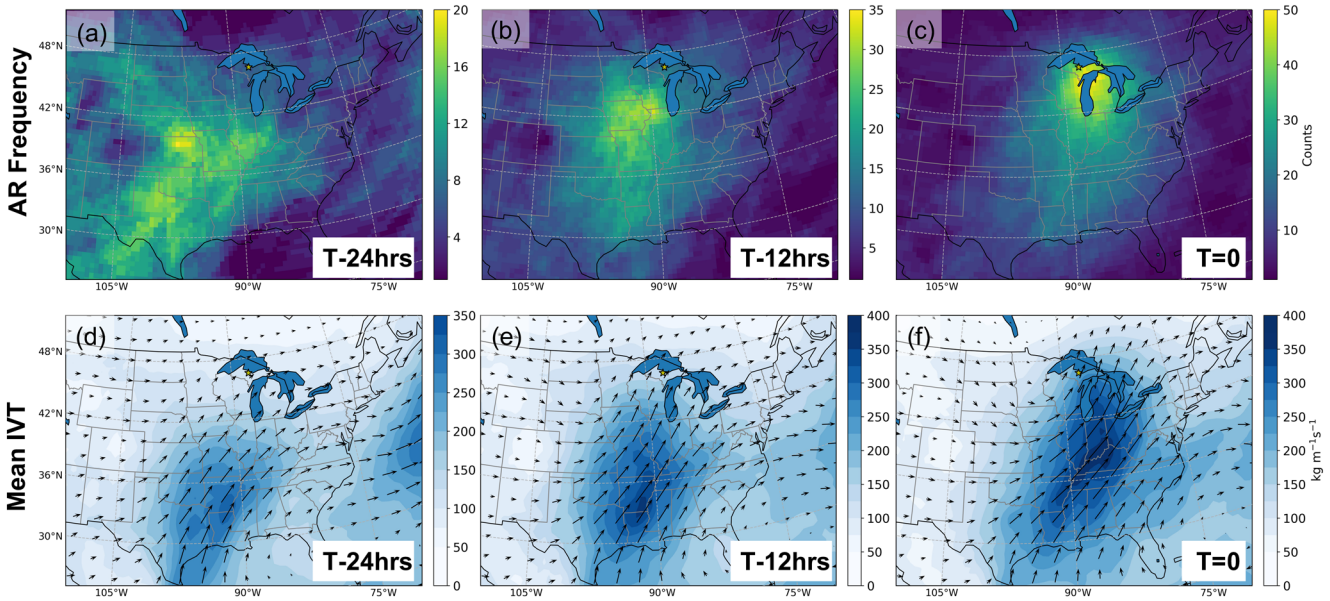


**Figure 2.** (a–c) Mean composites of atmospheric rivers identified by Mattingly et al. (2018) (a) 24 h before, (b) 12 h before, and (c) during a deep precipitation event coincident with an atmospheric river (AR) within 100 km of Marquette, Michigan. (d–f) Same as a-c but for mean composites of integrated vapor transport (IVT) values and associated mean moisture transport vectors.

the PDO (Mantua et al., 1997). The correlation with the PNA index is −0.28 using monthly AR frequency, while the correlation with the PDO index is −0.5 using seasonal AR frequency (November–April), with significance at the 95% level. The correlations of seasonal AR frequency with eastern Pacific ENSO and the AO are insignificant.

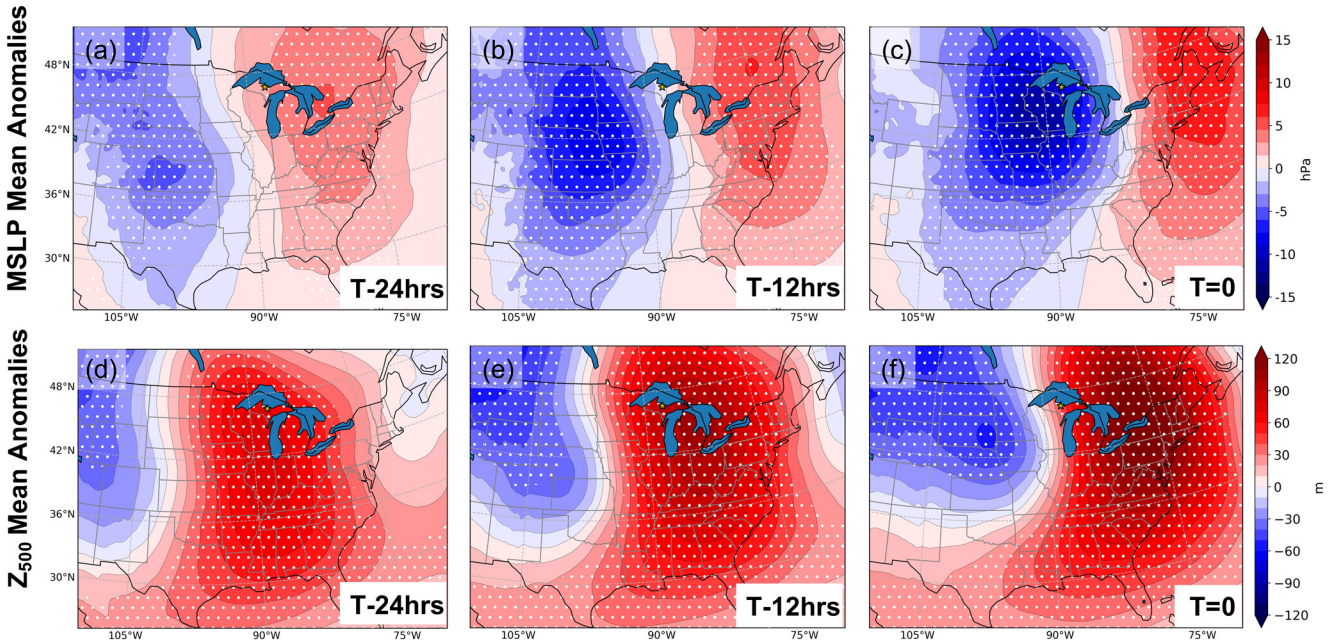


**Figure 3.** (a–c) Composite mean anomalies of ERA5 mean sea level pressure (MSLP) (a) 24 h before, (b) 12 h before, and (c) during a deep precipitation event coincident with an atmospheric river (AR). (d–f) Same as a-c but for composite mean anomalies of ERA5 500 hPa geopotential height ($Z_{500}$). White stippling represents statistical significance (95th percentile).

## 4. Discussion

The above results show that cold-season ARs occur 6.4% of the time, but are four times more common during deep precipitation events (28% frequency). Deep precipitation in the Upper Great Lakes region is synoptically-forced and generally moves in from south of the site (Kulie et al., 2021; Pettersen, Kulie, et al., 2020). Other studies in the central U.S. found that ARs causing extreme precipitation and flooding are embedded within synoptic systems originating from the southwest (Lavers & Villarini, 2013; Nayak et al., 2016). Recent work by Slinskey et al. (2020) determined that ARs in the Upper Great Lakes region generally come from the southwest, regardless of precipitation regime or season. During the cold season, we find that ARs are more likely to be present with no precipitation (4.9% frequency) than with shallow precipitation (3.9%). This is not entirely surprising as shallow precipitation events in Marquette are generally lake-effect, which are produced by cold-air outbreaks over relatively warm water (Niziol et al., 1995). Lake-effect precipitation traverses over Lake Superior from the north within high pressure (Kulie et al., 2021; Pettersen, Kulie, et al., 2020), which would deflect ARs and IVT impinging from the south. Additionally, AR precipitation is likely produced through vertically extensive lifting mechanisms such as isentropic ascent, frontal uplift, and occasional embedded convection, and prior studies have observed both stratiform and convective precipitation extends above 3 km in oceanic ARs (Cannon et al., 2020; Finlon et al., 2020). Therefore, the remainder of this discussion will focus on the impact of ARs during cold-season deep precipitation events.

The presence of an AR during cold-season deep precipitation events leads to increased rates (Table 1) and a higher likelihood that the precipitation phase will be rain at the surface. Enhanced precipitation is evidenced by both the PIP-retrieved rates and the observations of larger MRR reflectivity values (Figure 1a), as higher radar reflectivity can be indicative of larger and/or more massive hydrometeors, a greater number of particles, aggregation, riming, or a combination therein. This is consistent with prior studies that showed enhanced precipitation to be common during AR events (Guan et al., 2010; Neiman et al., 2012; Rivera et al., 2014; Slinskey et al., 2020; Warner et al., 2012). We found surface temperatures to be significantly warmer during deep precipitation events with an AR (+1.86°C). Cold-season rain occurs when snow and ice particles begin melting at a sufficiently high altitude, thus phasing to liquid before reaching the surface. ERA5 upper-level temperatures at Marquette during these events show anomalous warmth (850 hPa, mean anomaly of +4.0°C; 500 hPa, mean anomaly of +6.5°C), implying that the melting level may be higher in the atmosphere when there is an AR. Additionally, the MRR observations show a radar bright band for individual deep precipitation events (not shown), which indicates melting within the profile (Byers & Coons, 1947). The PIP indicates a significantly higher frequency of cold-season rain (20.1%) when an AR is present compared to when not (5.74%). Other studies have similarly found that cold-season ARs are associated with warmer lower tropospheric temperatures and higher melting levels during the cold season in the Sierra Nevada mountain range (Kim et al., 2013; Neiman et al., 2008), which leads to increased frequency of rain-on-snow events and consequent flooding (Guan et al., 2016). A fourfold increase in rain frequency in Marquette during cold-season AR-enhanced deep precipitation events also implies a higher occurrence of rain-on-snow events. The association of ARs with higher melting levels and more cold-season rain during deep precipitation events motivates the need to better track these features to aid forecasting and flood prediction in the Upper Great Lakes region.

The wind rose in Figure 1c and the IVT composites in Figure 2 demonstrate predominant south-southwesterly flow toward the site (>20% frequency) during these AR-enhanced deep precipitation events, which is consistent with previous work examining AR activity in the upper Midwest (Slinskey et al. 2020). ENE winds also occur (Figure 1c) when Marquette is in the northwest quadrant of a low-pressure system. When the backside of these systems traverse Lake Superior, deep precipitation can be further invigorated by open water surface, leading to "lake-enhanced" precipitation (Kulie et al., 2021). The AR composites in Figure 2 track northeastward toward the Upper Great Lakes region in the 24 h preceding a deep precipitation event, while simultaneously, anomalously low MSLP and $Z_{500}$ from the west deepen, and east of Marquette the MSLP and $Z_{500}$ are both anomalously high (Figure 3). This circulation pattern acts to draw moisture up from the Gulf of Mexico as well as enhance IVT and would support the development of synoptically-forced deep precipitation. The same east-west configuration of anomalous MSLP and trough-ridge setup with southwesterly flow during AR events is consistent with previous studies in the central U.S. (Lavers & Villarini, 2013; Nayak et al., 2016). This implies that these ARs will impact both the central U.S. and Upper

Great Lakes region, which is supported by the lagged composites shown in Figure 2. To our knowledge, the advection of moisture from the Gulf coinciding with and impacting cold-season deep precipitation has not been previously explored this far inland at higher latitudes.

Linking climate signals to AR frequency can aid in predictability of the risk associated with AR-enhanced deep precipitation events during the cold season in the Great Lakes region. The higher AR frequency during the negative phase of the PNA is consistent with findings from studies focused in the Sierra Nevada (Guan et al., 2013; Guan & Waliser, 2015) and central U.S. (Lavers & Villarini, 2013). The positive phase of the PDO has been found to be correlated with ARs impinging on the West Coast (Gershunov et al., 2017; Guirguis et al., 2019). However, the high correlation between AR frequency in the Midwest and the negative phase of the PDO has not been previously documented. More work is needed to better understand the connection to the PDO and its relevant processes (e.g., Newman et al., 2016). Seasonal AR frequency correlations with eastern Pacific ENSO as well as the AO were also computed, but were insignificant.

## 5. Concluding Remarks

This study finds a clear connection between atmospheric rivers in the Great Lakes region and deep, synoptically-driven precipitation events during the winter season. We leveraged an AR database that is sensitive to the relatively drier and colder conditions that occur inland and at northern mid-latitudes. We temporally matched ARs with ground-based precipitation and meteorological observations from the Marquette, Michigan NWS office. While the impact of ARs has been well-documented in coastal regions and the central U.S., few studies have identified AR patterns in the Great Lakes region. Despite being far inland, we identified an AR within 100 km of Marquette coincident with 28% of cold-season deep precipitation events. These AR-enhanced deep precipitation events experience higher precipitation rates and a fourfold increase in the likelihood of rain, compared to when an AR is not present. More rainfall indicates higher risk of rain-on-snow during an AR event and thus increased wintertime flooding.

The moisture associated with these ARs is advected primarily from southwest of the site, with a few instances of moisture advection from the west. The MSLP and $Z_{500}$ are anomalously low over the Great Lakes region during these AR-enhanced deep precipitation events, with significant anomalous ridging to the east. Upper-level temperature anomalies indicate that during an AR event the melting level is much higher, which is consistent with the tendency toward increased rain events. Further analysis found that climatologically, ARs within 100 km of Marquette occur more often during the negative phases of the PDO and PNA. While the PNA correlation with ARs has been linked in several other studies, the PDO correlation has not been before identified. The classification of the meteorological conditions and climate variability associated with ARs in the Upper Great Lakes region will aid in prediction of cold-season rain and flooding that impacts these communities, especially as global AR frequency and intensity change as a consequence of global warming (Espinoza et al., 2018).

**Acknowledgments**
This work was funded by NASA Grants NNX12AQ76G, 80NSSC18K0701, 80NSSC19K0712, and 80NSSC20K0982, and NOAA Grant NA15NES4320001. Thanks to the National Weather Service in Marquette, Michigan for hosting and maintaining the suite of instruments used in this work and sharing meteorological data with us. Thanks to the National Aeronautics and Space Administration Wallops Flight Facility and Goddard Flight Facility, as well as the Global Precipitation Measurement (GPM) program for providing the MRR and PIP instruments used in this work. The authors thank the Iowa Environmental Mesonet at Iowa State University for archiving meteorological data collected at Sawyer International Airport that are used to supplement missing data in February 2019 (this data included in Marquette, Michigan observational data set).

## Data Availability Statement

Meteorological ground-based data from Marquette, Michigan and the associated AR and IVT data set have been uploaded to a repository (doi: 10.5281/zenodo.4469817). NEXRAD data provided by the NOAA National Center for Environmental Information were accessed in August 2020 (doi: 10.7289/V5W9574V). ERA5 data used in this study were downloaded from the Copernicus Climate Data Store (CDS). Specifically, monthly and daily single-level (doi: 10.24381/cds.adbb2d47) and pressure-level (doi: 10.24381/cds.bd0915c6) data were accessed in October 2020. MERRA-2 data were downloaded from the NASA Goddard Earth Sciences Data and Information Services Center and were accessed in April 2020. The NOAA CPC provides climate variability indices.

## References

Bolsenga, S. J., & Norton, D. C. (1992). Maximum snowfall at long-term stations in the US/Canadian Great Lakes. *Natural Hazards*, *5*, 221–232. https://doi.org/10.1007/bf00125228

Byers, H. R., & Coons, R. D. (1947). The "bright line" in radar cloud echoes and its probable explanation. *Journal of Meteorology*, *4*, 75–81. https://doi.org/10.1175/1520-0469(1947)004%3C0078:TLIRCE%3E2.0.CO;2

Byun, K., Chiu, C. M., & Hamlet, A. F. (2019). Effects of 21st century climate change on seasonal flow regimes and hydrologic extremes over the Midwest and Great Lakes region of the US. *Science of the Total Environment*, *650*, 1261–1277. https://doi.org/10.1016/j.scitotenv.2018.09.063

C3S. (2017). *ERA5: Fifth generation of ECMWF atmospheric reanalyses of the global climate*. Copernicus Climate Change Service Climate data Store. Retrieved from https://cds.climate.copernicus.eu/cdsapp#!/home

Cannon, F., Cordeira, J. M., Hecht, C. W., Norris, J. R., Michaelis, A., Demirdjian, R., & Ralph, F. M. (2020). GPM Satellite radar observations of precipitation mechanisms in atmospheric rivers. *Monthly Weather Review*, *148*(4), 1449–1463. https://doi.org/10.1175/MWR-D-19-0278.1

Changnon, S. A., Jr (1979). How a severe winter impacts on individuals. *Bulletin of the American Meteorological Society*, *60*, 110–114. https://doi.org/10.1175/1520-0477(1979)060%3C0110:HASWIO%3E2.0.CO;2

Espinoza, V., Waliser, D. E., Guan, B., Lavers, D. A., & Ralph, F. M. (2018). Global analysis of climate change projection effects on atmospheric rivers. *Geophysical Research Letters*, *45*, 4299–4308. https://doi.org/10.1029/2017GL076968

Finlon, J. A., Rauber, R. M., Wu, W., Zaremba, T. J., McFarquhar, G. M., Nesbitt, S. W., et al. (2020). Structure of an Atmospheric river over Australia and the Southern Ocean: II. Microphysical evolution. *Journal of Geophysical Research: Atmospheres*, *125*, e2020JD032514. https://doi.org/10.1029/2020JD032514

Gelaro, R., McCarty, W., Suárez, M. J., Todling, R., Molod, A., Takacs, L., et al. (2017). The modern-era retrospective analysis for research and applications, Version 2 (MERRA-2). *Journal of Climate*, *30*, 5419–5454. https://doi.org/10.1175/JCLI-D-16-0758.1

Gershunov, A., Shulgina, T., Ralph, F. M., Lavers, D. A., & Rutz, J. J. (2017). Assessing the climate-scale variability of atmospheric rivers affecting western North America. *Geophysical Research Letters*, *44*, 7900–7908. https://doi.org/10.1002/2017GL074175

Goldenson, N., Leung, L. R., Bitz, C. M., & Blanchard-Wrigglesworth, E. (2018). Influence of atmospheric rivers on mountain snowpack in the western United States. *Journal of Climate*, *31*(24), 9921–9940. https://doi.org/10.1175/JCLI-D-18-0268.1

Gorodetskaya, I. V., Tsukernik, M., Claes, K., Ralph, F. M., Neff, W. D., & Van Lipzig, N. P. M. (2014). The role of atmospheric rivers in anomalous snow accumulation in East Antarctica. *Geophysical Research Letters*, *41*, 6199–6206. https://doi.org/10.1002/2014GL060881

Guan, B., Molotch, N. P., Waliser, D. E., Fetzer, E. J., & Neiman, P. J. (2010). Extreme snowfall events linked to atmospheric rivers and surface air temperature via satellite measurements. *Geophysical Research Letters*, *37*(20), L20401. https://doi.org/10.1029/2010GL044696

Guan, B., Molotch, N. P., Waliser, D. E., Fetzer, E. J., & Neiman, P. J. (2013). The 2010/2011 snow season in California's Sierra Nevada: Role of atmospheric rivers and modes of large-scale variability. *Water Resources Research*, *49*(10), 6731–6743. https://doi.org/10.1002/wrcr.20537

Guan, B., & Waliser, D. E. (2015). Detection of atmospheric rivers: Evaluation and application of an algorithm for global studies. *Journal of Geophysical Research: Atmospheres*, *120*(24), 12514–12535. https://doi.org/10.1002/2015JD024257

Guan, B., Waliser, D. E., Molotch, N. P., Fetzer, E. J., & Neiman, P. J. (2012). Does the Madden–Julian oscillation influence wintertime atmospheric rivers and snowpack in the Sierra Nevada? *Monthly Weather Review*, *140*(2), 325–342. https://doi.org/10.1175/MWR-D-11-00087.1

Guan, B., Waliser, D. E., Ralph, F. M., Fetzer, E. J., & Neiman, P. J. (2016). Hydrometeorological characteristics of rain-on-snow events associated with atmospheric rivers. *Geophysical Research Letters*, *43*, 2964–2973. https://doi.org/10.1002/2016GL067978

Guirguis, K., Gershunov, A., Shulgina, T., Clemesha, R. E. S., & Ralph, F. M. (2019). Atmospheric rivers impacting Northern California and their modulation by a variable climate. *Climate Dynamics*, *52*, 6569–6583. https://doi.org/10.1007/s00382-018-4532-5

Hersbach, H., Bell, B., Berrisford, P., Hirahara, S., Horányi, A., Muñoz-Sabater, J., et al. (2020). The ERA5 global reanalysis. *Quarterly Journal of the Royal Meteorological Society*, *146*, 1999–2049. https://doi.org/10.1002/qj.3803

Kim, J., Waliser, D. E., Neiman, P. J., Guan, B., Ryoo, J. M., & Wick, G. A. (2013). Effects of atmospheric river landfalls on the cold season precipitation in California. *Climate Dynamics*, *40*, 465–474. https://doi.org/10.1007/s00382-012-1322-3

Klugmann, D., Heimsohn, K., & Kirtzel, H. J. (1996). A low cost 24 GHz FM-CW Doppler radar rain profiler. *Contributions to Atmospheric Physics*, *61*, 247–253.

Kulie, M. S., Pettersen, C., Merrelli, A. J., Wagner, T. J., Wood, N. B., Dutter, M., et al. (2021). Snowfall in the Northern Great Lakes: Lessons learned from a Multi-Sensor Observatory. *Bulletin of the American Meteorological Society*. https://doi.org/10.1175/BAMS-D-19

Lavers, D. A., & Villarini, G. (2013). Atmospheric rivers and flooding over the central United States. *Journal of Climate*, *26*(20), 7829–7836. https://doi.org/10.1175/JCLI-D-13-00212.1

Mahoney, K., Jackson, D. L., Neiman, P., Hughes, M., Darby, L., Wick, G., et al. (2016). Understanding the role of atmospheric rivers in heavy precipitation in the southeast United States. *Monthly Weather Review*, *144*(4), 1617–1632. https://doi.org/10.1175/MWR-D-15-0279.1

Mantua, N. J., Hare, S. R., Zhang, Y., Wallace, J. M., & Francis, R. C. (1997). A Pacific Interdecadal Climate Oscillation with impacts on salmon production. *Bulletin of the American Meteorological Society*, *78*(6), 1069–1079. https://doi.org/10.1175/1520-0477(1997)078%3C1069:APICOW%3E2.0.CO;2

Mattingly, K. S., Mote, T. L., & Fettweis, X. (2018). Atmospheric river impacts on Greenland Ice Sheet surface mass balance. *Journal of Geophysical Research: Atmospheres*, *123*, 8538–8560. https://doi.org/10.1029/2018JD028714

McCabe, G. J., Clark, M. P., & Hay, L. E. (2007). Rain-on-snow events in the western United States. *Bulletin of the American Meteorological Society*, *88*, 319–328. https://doi.org/10.1175/BAMS-88-3-319

Miller, D. K., Hotz, D., Winton, J., & Stewart, L. (2018). Investigation of atmospheric rivers impacting the Pigeon River Basin of the Southern Appalachian Mountains. *Weather and Forecasting*, *33*(1), 283–299. https://doi.org/10.1175/WAF-D-17-0060.1

Miller, D. K., Miniat, C. F., Wooten, R. M., & Barros, A. P. (2019). An expanded investigation of atmospheric Rivers in the Southern Appalachian Mountains and their connection to landslides. *Atmos*, *10*(2), 71. https://doi.org/10.3390/atmos10020071

Moore, B. J., Neiman, P. J., Ralph, F. M., & Barthold, F. E. (2012). Physical processes associated with heavy flooding rainfall in Nashville, Tennessee, and vicinity during 1–2 May 2010: The role of an atmospheric river and mesoscale convective systems. *Monthly Weather Review*, *140*(2), 358–378. https://doi.org/10.1175/MWR-D-11-00126.1

Mundhenk, B. D., Barnes, E. A., Maloney, E. D., & Nardi, K. M. (2016). Modulation of atmospheric rivers near Alaska and the U.S. West Coast by northeast Pacific height anomalies. *Journal of Geophysical Research: Atmospheres*, *121*, 12751–12765. https://doi.org/10.1002/2017JD025350

Nayak, M. A., Villarini, G., & Bradley, A. A. (2016). Atmospheric rivers and rainfall during NASA's Iowa Flood Studies (IFloodS) campaign. *Journal of Hydrometeorology*, *17*(1), 257–271. https://doi.org/10.1175/JHM-D-14-0185.1

Neiman, P. J., Ralph, F. M., Moore, B. J., Hughes, M., Mahoney, K. M., Cordeira, J. M., & Dettinger, M. D. (2012). The landfall and inland penetration of a flood-producing atmospheric river in Arizona. Part I: Observed synoptic-scale, orographic, and hydrometeorological characteristics. *Journal of Hydrometeorology*, *14*, 460–484. https://doi.org/10.1175/JHM-D-12-0101.1

Neiman, P. J., Ralph, F. M., Wick, G. A., Lundquist, J. D., & Dettinger, M. D. (2008). Meteorological characteristics and overland precipitation impacts of atmospheric rivers affecting the West Coast of North America based on eight years of SSM/I satellite observations. *Journal of Hydrometeorology*, *9*(1), 22–47. https://doi.org/10.1175/2007JHM855.1

Newman, A. J., Kucera, P. A., & Bliven, L. F. (2009). Presenting the snowflake video imager (SVI). *Journal of Atmospheric and Oceanic Technology*, *26*(2), 167–179. https://doi.org/10.1175/2008JTECHA1148.1

Newman, M., Alexander, M. A., Ault, T. R., Cobb, K. M., Deser, C., Di Lorenzo, E., et al. (2016). The Pacific Decadal Oscillation, Revisted. *Journal of Climate*, *29*, 4399–4427. https://doi.org/10.1175/JCLI-D-15-0508.1

Niziol, T. A., Snyder, W. R., & Waldstreicher, J. S. (1995). Winter weather forecasting throughout the eastern United States. Part IV: Lake effect snow. *Weather and Forecasting*, *10*, 61–77. https://doi.org/10.1175/1520-0434(1995)010%3C0061:WWFTTE%3E2.0.CO;2

Norton, D. C., & Bolsenga, S. J. (1993). Spatiotemporal trends in lake effect and continental snowfall in the Laurentian Great Lakes, 1951–1980. *Journal of Climate*, *6*, 1943–1956. https://doi.org/10.1175/1520-0442(1993)006%3C1943:STILEA%3E2.0.CO;2

Papineau, J., & Holloway, E. (2012). *The dry side of atmospheric rivers in Alaska, Anchorage Forecast Office Research Papers*. NOAA/NWS/ARH. Retrieved from http://citeseerx.ist.psu.edu/viewdoc/summary?doi=10.1.1.729

Pettersen, C., Bliven, L. F., Kulie, M. S., Wood, N. B., Shates, J. A., Anderson, J., et al. (2021). The precipitation imaging package: Phase partitioning capabilities. *Remote Sensing*, *13*, 2183. https://doi.org/10.3390/rs13112183

Pettersen, C., Bliven, L. F., von Lerber, A., Wood, N. B., Kulie, M. S., Mateling, M. E., et al. (2020). The Precipitation imaging package: Assessment of microphysical and bulk characteristics of snow. *Atmos*, *11*, 785. https://doi.org/10.3390/atmos11080785

Pettersen, C., Kulie, M. S., Bliven, L. F., Merrelli, A. J., Petersen, W. A., Wagner, T. J., et al. (2020). A composite analysis of snowfall modes from four winter seasons in Marquette, Michigan. *Journal of Applied Meteorology and Climatology*, *59*, 103–124. https://doi.org/10.1175/JAMC-D-19-0099.1

Riebsame, W. E., Diaz, H. F., Moses, T., & Price, M. (1986). The social burden of weather and climate hazards. *Bulletin of the American Meteorological Society*, *67*, 1378–1388. https://doi.org/10.1175/1520-0477(1986)067%3C1378:TSBOWA%3E2.0.CO;2

Rivera, E. R., Dominguez, F., & Castro, C. L. (2014). Atmospheric rivers and cool season extreme precipitation events in the Verde River basin of Arizona. *Journal of Hydrometeorology*, *15*(2), 813–829. https://doi.org/10.1175/JHM-D-12-0189.1

Rutz, J. J., Shields, C. A., Lora, J. M., Payne, A. E., Guan, B., Ullrich, P., et al. (2019). The atmospheric river tracking method intercomparison project (ARTMIP): Quantifying uncertainties in atmospheric river climatology. *Journal of Geophysical Research: Atmospheres*, *124*, 13777–13802. https://doi.org/10.1029/2019JD030936

Rutz, J. J., Steenburgh, W. J., & Ralph, F. M. (2014). Climatological characteristics of atmospheric rivers and their inland penetration over the western United States. *Monthly Weather Review*, *142*(2), 905–921. https://doi.org/10.1175/MWR-D-13-00168.1

Slinskey, E. A., Loikith, P. C., Waliser, D. E., Guan, B., & Martin, A. (2020). A climatology of atmospheric rivers and associated precipitation for the seven U.S. National Climate Assessment Regions. *Journal of Hydrometeorology*, *21*, 2439–2456. https://doi.org/10.1175/JHM-D-20-0039.s1

Waliser, D., & Guan, B. (2017). Extreme winds and precipitation during landfall of atmospheric rivers. *Nature Geoscience*, *10*(3), 179–183. https://doi.org/10.1038/NGEO2894

Wallace, J. M., & Gutzler, D. S. (1981). Teleconnections in the geopotential height field during the Northern Hemisphere winter. *Monthly Weather Review*, *109*(4), 784–812. https://doi.org/10.1175/1520-0493(1981)109%3C0784:TITGHF%3E2.0.CO;2

Warner, M. D., Mass, C. F., & Salathé, E. P., Jr. (2012). Wintertime extreme precipitation events along the Pacific Northwest coast: Climatology and synoptic evolution. *Monthly Weather Review*, *140*(7), 2021–2043. https://doi.org/10.1175/MWR-D-11-00197.1

Wilks, D. S. (2011). *Statistical methods in the atmospheric sciences* (3rd ed.). Cambridge, MA: Academic Press.

Zhu, Y., & Newell, R. E. (1998). A proposed algorithm for moisture fluxes from atmospheric rivers. *Monthly Weather Review*, *126*(3), 725–735. https://doi.org/10.1175/1520-0493(1998)126%3C0725:APAFMF%3E2.0.CO;2